Toward improved corrections for radiation-induced biases in radiosonde temperature observations

Bomin Sun,[1] Anthony Reale,[2] Steven Schroeder,[3] Dian J. Seidel,[4] and Bradley Ballish[5]

Received 24 October 2012; revised 22 March 2013; accepted 26 March 2013; published 28 May 2013.

[1] Radiation-induced biases in global operational radiosonde temperature data from May 2008 to August 2011 are examined by using spatially and temporally collocated Constellation Observing System for Meteorology, Ionosphere, and Climate (COSMIC) data as estimates of the truth. The data on average from most radiosonde types show a nighttime cold bias and a daytime warm bias relative to COSMIC. Most daytime biases increase with altitude and solar elevation angle (SEA). The global average biases in the 15–70 hPa layer are -0.05 ± 1.89 K standard deviation (~52,000 profiles) at night and 0.39 ± 1.80 K standard deviation (~64,500 profiles) in daytime (SEA $> 7.5°$). Daytime warm biases associated with clouds are smaller than those under clear conditions. Newer sondes (post-2000) have smaller biases and appear to be less sensitive to effects of clouds. Biases at night show greater seasonal and zonal variations than those for daytime. In general, warm night biases are associated with warm climate regimes and less warm or cold night biases with cold climate regimes. Bias characteristics for 13 major radiosonde types are provided, as a basis for updating radiosonde corrections used in numerical weather predictions, for validating satellite retrievals, and for adjusting archived radiosonde data to create consistent climate records.

Citation: Sun, B., A. Reale, S. Schroeder, D. J. Seidel, and B. Ballish (2013), Toward improved corrections for radiation-induced biases in radiosonde temperature observations, *J. Geophys. Res. Atmos.*, *118*, 4231–4243, doi:10.1002/jgrd.50369.

1. Introduction

[2] Upper air temperature, pressure, humidity, and wind observations have been made by balloon-borne radiosonde instruments for over 7 decades and have had important applications in weather prediction, upper air climate research, and satellite data calibration and validation. However, measurement biases undermine their value in all of these applications, and various approaches have been taken to correct them [e.g., *Teweles and Finger*, 1960; *Tarbell and Tower*, 1980; *Uddstrom*, 1984; *McMillin et al.*, 1988, 1992; *Luers and Eskridge*, 1995, 1998; *Lanzante et al.*, 2003; *Free et al.*, 2004; *Haimberger et al.*, 2008; *Sherwood et al.*, 2008; *Christy and Norris*, 2009; *Thorne et al.*, 2011]. Here we present an analysis of temperature biases in radiosonde observations (RAOBs), with the intention of facilitating improvements in correction techniques.

[3] Radiosonde temperature biases, where the sensor temperature differs from the air temperature, are mainly caused by radiative effects (typically a warm daytime bias from sunlight heating the sensor and a cold bias at night as the sensor emits longwave radiation) with smaller errors due to lags in sensor response to changing temperatures as the radiosonde rises. All factors affecting longwave and shortwave fluxes around the sensor influence the bias, including sensor physical characteristics and mounting, and environmental factors including surface temperature, solar elevation angle (SEA), temperature lapse rate, ventilation velocity, and clouds [e.g., *McMillin et al.*, 1992; *Luers and Eskridge*, 1995, 1998; *Bower and Fitzgibbon*, 2003, 2004; *Mattioli et al.*, 2007].

[4] Most soundings transmitted through the Global Telecommunication System (GTS), and used in this study, contain radiation corrections applied at each site to attempt to compensate for the biases, based on algorithms provided by radiosonde manufacturers or national meteorological agencies. Because the algorithms were derived using limited data and most adjustments are a function of only a few factors (generally pressure level, SEA, and balloon ascent speed), corrections might be too small or large, so biases remain even in "corrected" temperature measurements [e.g., *Gaffen*, 1994; *Sherwood et al.*, 2005; *Randel and Wu*, 2006; *Haimberger et al.*, 2008]. Most forecast centers, including NOAA's National Centers for Environmental

[1]I. M. Systems Group, Inc. at NOAA Center for Satellite Applications and Research, College Park, Maryland, USA.
[2]NOAA Center for Satellite Applications and Research, College Park, Maryland, USA.
[3]Department of Atmospheric Sciences, Texas A&M University, College Station, Texas, USA.
[4]NOAA Air Resources Laboratory, College Park, Maryland, USA.
[5]NOAA NCEP Environmental Modeling Center, College Park, Maryland, USA.

Corresponding author: B. Sun, IMSG at NOAA Center for Satellite Applications and Research, NCWCP, 5830 University Research Court, Office #2825, College Park, MD 20740, USA. (bomin.sun@noaa.gov)

2169-897X/13/10.1002/jgrd.50369

Prediction (NCEP), develop and apply additional corrections for each radiosonde type to compensate for remaining biases when ingesting GTS soundings into forecast models. This study does not use sounding data incorporating NCEP corrections, but a major goal is to better quantify radiosonde biases to develop future improved corrections.

[5] Using the phase delay of radio waves transmitted by Global Positioning System (GPS) satellites as they pass through the Earth's atmosphere, high-resolution vertical profiles of the atmospheric structure can be derived in all weather conditions [*Kursinski et al*., 1997; *Hajj et al*., 2002]. Dry temperature (T_d) is one of the variables derived from GPS radio occultation (RO) measurements, and its average accuracy is < 0.1 K where water vapor is negligible [*Hajj et al*., 2004]. By intercomparing GPSRO products of 2002–2008 from five data processing centers, *Ho et al*. [2012] found out that four T_d data products are consistent within ~ 0.1 K relative to the mean in the 8–30 km layer. The high accuracy of GPSRO T_d has been shown to be of value in assessing the quality of temperature measurements of other observing systems by several previous studies [*Kuo et al*., 2005; *Ho et al*., 2007; *He et al*., 2009].

[6] This study employs over 3 years (May 2008 to August 2011) of GPSRO data as a reference to assess and quantify temperature biases for the global operational radiosonde network. While *Kuo et al*. [2005] and *He et al*. [2009] analyzed the temperature biases at the upper troposphere and lower stratosphere (UTLS) in three to four sonde types, this work evaluates the biases for 13 different sonde types, which account for 92% of global reports. The RO data used in this study are from the University Corporation for Atmospheric Research (UCAR) Constellation Observing System for Meteorology, Ionosphere, and Climate (COSMIC) [*Anthes et al*., 2008]. In section 2, we describe the basic characteristics of radiosonde and collocated COSMIC data. Using COSMIC as a reference, section 3 presents the RAOB-minus-COSMIC temperature differences at different SEAs, for both individual sonde types and the global radiosonde network, and the zonal and seasonal variations and radiative impact of clouds are also evaluated for the global data. Section 4 presents radiosonde radiation error impact in numerical weather prediction (NWP) data assimilation, and section 5 is devoted to conclusions and discussion.

2. Data

[7] Radiosonde and collocated COSMIC data are collected with the NOAA Products Validation System (NPROVS) operated at the NOAA/National Environmental Satellite, Data, and Information Service (NESDIS) Center for Satellite Applications and Research [*Reale et al*., 2012]. NPROVS provides a centralized, integrated near-real-time monitoring and validation function for intercomparing satellite-derived temperature and water vapor sounding products against collocated global radiosonde and dropsonde observations and NWP products.

[8] The NPROVS collocation approach considers the spatial and temporal aspects of each satellite platform to ensure consistent and robust selection of a single "closest" sounding from each satellite product that lies within 6 h and 250 km of a given RAOB [*Sun et al*., 2010; *Reale et al*., 2012]. NPROVS began routine collocations of global RAOBs with satellite sounding products in 2008, and data from May 2008 to August 2011 are used in the analysis.

2.1. Radiosonde Data

[9] RAOBs in NPROVS collocations are those assimilated operationally by NOAA's NCEP (http://www.emc.ncep.noaa.gov/mmb/data_processing/prepbufr.doc/document.htm). In addition to the mandatory and significant level report data for temperature, dew point temperature, and wind, quality control (QC) markers of these variables determined during the gross error check of the NCEP Global Forecast System (GFS) 6 h forecast data assimilation [*Collins*, 2001a, 2001b] and ancillary information, such as balloon drift and collocated NWP data, are included for each RAOB. These RAOBs are then treated as the "anchor" for compiling NPROVS collocated satellite observations. Note that while this study considers the NCEP quality control results, it uses GTS soundings, which include site radiation corrections but not NCEP corrections.

[10] We rejected observations rejected by the NCEP assimilation system or having temperature difference 15 K from the NCEP background, as well as those with a vertical extent < 5 km or a vertical gap ≥ 4 km, totaling ~3% of the observations. About 187,000 soundings from 721 land stations and 27 ships were used. Approximately 68% are from Northern Hemisphere midlatitude land areas.

[11] Radiosonde instrument types, their radiation corrections, and their tracking codes are identified in the "31313 group" of the RAOB report in over 80% of worldwide soundings since the late 1990s. Sounding stations in China, most stations in India, and a few stations in other locations do not report the 31313 group or started reporting after 2008. Figure 1 shows the spatial distribution of major radiosonde types, and Table 1 summarizes their characteristics. Vaisala RS92 (red circles) is the most widely used in this period. Many countries use their own sonde types: Sippican in the U.S., MRZ in Russia, Shang-E in China, and IMD in India. Although all sensors have lag errors, few operational radiosonde types apply lag corrections, and the World Meteorological Organization (WMO) does not define any variable to report if a lag correction is applied.

[12] For most sonde types, corrections for radiation error were applied at the site before the data were transmitted. Some are only solar radiation corrections, while others are solar and infrared radiation corrections. Sippican-B2 (VIZ-B2 until December 1997) is an exception; no corrections are applied at sites.

[13] The 31313 group does not identify a changed correction at a station if the new and old corrections have the same type (such as automatic solar correction). For example, since their introduction in 1981 and 2003, respectively, there have been several versions of the corrections to Vaisala RS80 and RS92 (see section 3.2), and the dates of implementation can vary from station to station. This analysis uses data for 2008–2011 and therefore reflects whatever correction algorithms were in place during that period.

2.2. COSMIC Data

[14] The COSMIC data used in this study are from the University Corporation for Atmospheric Research (UCAR) COSMIC Data Analysis and Archive Center (http://www.

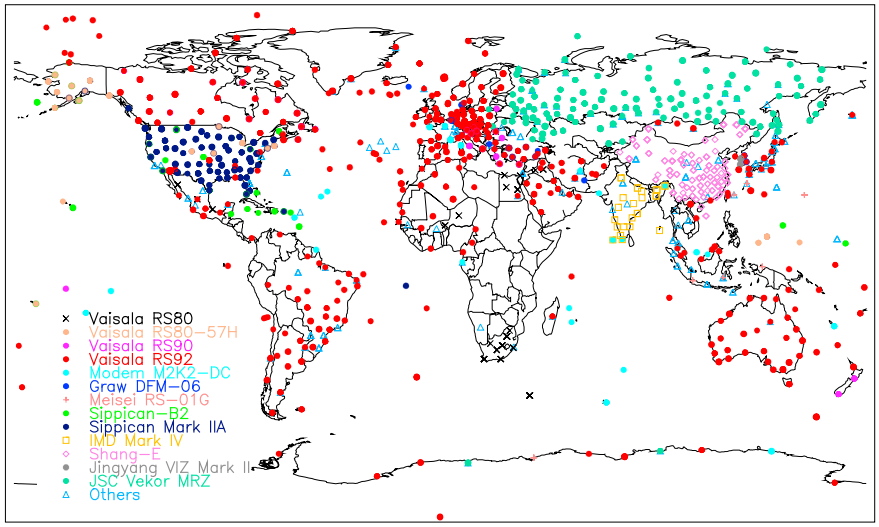

Figure 1. Global distribution of radiosonde stations and ship reports collocated within 6 h and 250 km of COSMIC soundings for May 2008 to August 2011. See Table 1 for more information of radiosonde types (denoted with different colors) analyzed.

cosmic.ucar.edu/cdaac) near-real-time processing, available within a few hours of the measurements, and incorporated in NPROVS. Postprocessed data products, generated using a fixed processing algorithm and so more suitable for climate studies, are also available. *Ho et al.* [2012] revealed that UCAR postprocessed T_d at 8–30 km is 0.03 ± 0.43 K different from the mean value averaged from five products compared. Using 13 days of data available to us, we found the differences between UCAR near-real-time and postprocessed T_d averaged from data at global radiosonde sites (see Figure 1) are 0.05 ± 0.61 K (values after reported throughout the paper are standard deviations) at 15–100 hPa and 0.01 ± 0.68 K at 15–70 hPa. These small differences assure us that UCAR near-real-time T_d can be used as a reference to assess the UTLS biases in radiosonde data.

[15] COSMIC provides wet T (T_w) profiles in addition to T_d. COSMIC T_w and water vapor profiles are developed using the COSMIC bending angle or refractivity measurements in conjunction with one-dimensional variational analysis method (1DVar; see http://cosmic-io.cosmic.ucar.edu/cdaac/doc/documents/1dvar.pdf for details). The near-real-time COSMIC retrieval profiles are generated using the NCEP 12 h forecast as the first guess, which are retained on the product files. Retrievals of T_w in the upper troposphere and stratosphere are expected to be accurate because the moisture affecting on GPSRO bending angle measurements is small. In the low and middle troposphere, T_w and water vapor retrievals are interdependent and strongly dependent on the first guess, but as will be shown in section 3.2, T_w still can be used to detect tropospheric temperature measurement anomalies in some sonde types.

Table 1. Characteristics of Major Radiosonde Types Used in the Study[a]

Type	Manufacturer	Country of Manufacture	Temperature Sensor	Site Radiation Correction	BUFR Code (Subtype)	Number of Reports	Percent of Global Reports	Approximate Year Introduced
RS80	Vaisala	Finland	Bead thermocap	Solar & IR	061, 067	3965	2.1%	1981
RS80-57H	Vaisala	Finland	Bead thermocap	Solar & IR	052	3302	1.8%	1998
RS90	Vaisala	Finland	Thin-wire F-Thermocap	Solar & IR	071	4017	2.1%	1995
RS92	Vaisala	Finland	Thin-wire F-Thermocap	Solar & IR	079, 080, 081	71,503	38.2%	2003
M2K2-DC	Modem	France	Bead or chip thermistor	Solar & IR	057	4882	2.6%	2006
DFM-06	Graw	Germany	Bead thermistor	Solar	017	1887	1.0%	2006
RS-01G	Meisei	Japan	Rod thermistor	Solar	055	1194	0.6%	2001
Sippican-B2	Sippican	U.S.	Rod thermistor	None	051	4938	2.6%	1997
Sippican Mark IIA	Sippican	U.S.	Chip thermistor	Solar	087	20,958	11.2%	2003
Mark IV	IMD	India	Rod thermistor	Solar or none	020	974	0.5%	2003
Shang-E	three manufacturers	China	Rod thermistor	Solar & IR	131, 132, 133	12,409	6.6%	2002
VIZ Mark II	Jinyang	Korea	Rod thermistor	Solar	021	719	0.4%	1987
MRZ	JSC Vektor	Russia	Rod thermistor	Solar	027, 058, 075, 088, 089	41,841	22.4%	1986

[a]Numbers of reports are based on collocations with COSMIC within 3 h and 250 km for May 2008 to August 2011 (see Figure 1).

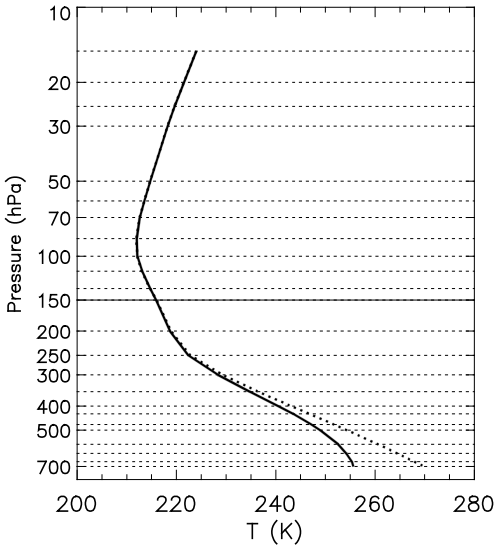

Figure 2. Average COSMIC dry temperature (solid curve) and retrieved or wet temperature (dotted curve) for all collocated profiles during May 2008 to August 2011. The thin solid line at 150 hPa separates the region (15 to 150 hPa) for which dry temperature was used to evaluate radiosonde data from the region (below 150 hPa) for which wet temperature was used. Radiosonde and COSMIC profiles are interpolated to the pressure levels indicated by dashed lines for analysis.

[16] Other sources of uncertainty in lower tropospheric retrievals include the presence of superrefraction or negative refractivity bias arising from sharp vertical gradients in water vapor [*Sokolovskiy*, 2003; *Ao*, 2007] and RO signal blockage in regions of high terrain. To minimize the influence of these height-dependent uncertainties in T_d and T_w, this study uses T_d at altitudes between 150 and 15 hPa and T_w between 700 and 150 hPa to form COSMIC T profiles at 24 fixed pressure levels (see Figure 2) for evaluating biases in radiosonde profiles and so emphasize the upper troposphere and low stratosphere where radiation biases are greatest and T_d is highly accurate.

3. Results

[17] The mean RAOB-minus-COSMIC temperature difference ($\overline{\Delta T}$) and its standard deviation ($SD_{\Delta T}$) are used to quantify RAOB temperature biases. These are computed for four SEA classes: NIGHT (SEA $< -7.5°$), DUSK/DAWN (SEA of $-7.5°$~$7.5°$), LOW (SEA of $7.5°$~$22.5°$), and HIGH (SEA $> 22.5°$). Statistics are also computed for ALL (all SEAs) and DAY (SEA $> 7.5°$) to facilitate the understanding of overall RAOB biases. Because spatial and temporal mismatch between RAOB and COSMIC profiles affects $SD_{\Delta T}$, but not $\overline{\Delta T}$ [*Sun et al.*, 2010], collocations within 3 h and 250 km are used here to minimize $SD_{\Delta T}$ and allow more consistent evaluation of $\overline{\Delta T}$.

[18] Note the actual sample sizes used to compute the bias statistics ($\overline{\Delta T}$ and $SD_{\Delta T}$) for individual sonde types and global data as well generally decrease with height above the upper troposphere due to the absence of valid radiosonde measurements. For example, the sample size for Vaisala RS92 is reduced to 54,107 for 15–70 hPa from 71,503 for the troposphere.

[19] The $\overline{\Delta T}$ values in the low stratosphere for most of the sonde types and global data are found to be significantly different from zero at the 0.05 or better level, even though their $SD_{\Delta T}$ values are relatively large, as indicated in Table 3 that summarizes the bias statistics. Statistical significance is also indicated in the text on the values of the bias differences when discussing older and new sondes, zonal and seasonal variations, and cloud effects.

[20] This section presents results first for specific sonde types, for direct applications to the bias correction problem, and then for the global network, including all sonde types and separately for newer and older types, to get the sense of biases in global data.

3.1. Individual Sonde Types

[21] This section shows the temperature bias analysis result for each of the 13 different sonde types, with emphasis on Vaisala RS92, the most widely used type; MRZ, the second most widely used type which shows unique $\overline{\Delta T}$ features; and Sippican-B2 for which no radiation corrections are applied at sites.

[22] *Vaisala RS92*. Three versions of Vaisala RS92 radiation corrections (1996, 2005, and 2010) have been used since its introduction to the upper air observing network and are available at the Vaisala sounding data continuity Web page http://www.vaisala.com/weather/products/datacontinuity.html. Over time, the corrections have generally increased in magnitude. For example, the 1996, 2005, and 2010 corrections at 20 hPa for 45° SEA are 0.33, 0.50, and 0.60 K (subtracted from raw radiosonde temperatures), respectively. The May 2008 to August 2011 data used here probably reflect the 2005 version of the correction algorithm, but generally, no documentation is available stating when a station upgrades software to use a more recent correction. In 2012 (after this study period), the U.S. National Weather Service (NWS)-supported Caribbean stations started using Vaisala RS92-D (code 183) radiosondes with no radiosonde corrections, and some other NWS stations started using RS92-NGP (code 152) radiosondes with the 2005 (not 2010) solar and infrared radiation correction version (W. Blackmore, NWS, personal communication, 2012).

[23] As shown in Figure 3, Vaisala RS92 shows a warm bias in the low stratosphere that increases with height and SEA. The mean biases for 15–70 hPa are 0.21 K for class ALL and 0.46 K for class HIGH. A slight warm bias (0.07 K for 15–70 hPa) also emerges for NIGHT. A "cold" bias (0.1–0.2 K) is present in Vaisala RS92 in the middle and upper troposphere, which is not found in many other sonde types (Figures 5–7). We have no explanation for the source of this bias.

[24] The seasonal pattern of $\overline{\Delta T}$ for Vaisala RS92 is shown in Figure 4. The summer and winter daytime $\overline{\Delta T}$ are similar for higher SEAs. But, for NIGHT and DUSK/DAWN, the summer $\overline{\Delta T}$ values exceed the winter ones by 0.22 K at 15–70 hPa, which is statistically significant at better than the 0.05 level.

[25] There are three subtypes of Vaisala RS92: DigiCora I, II, or Marwin (radiosonde code 079), DigiCora III (code

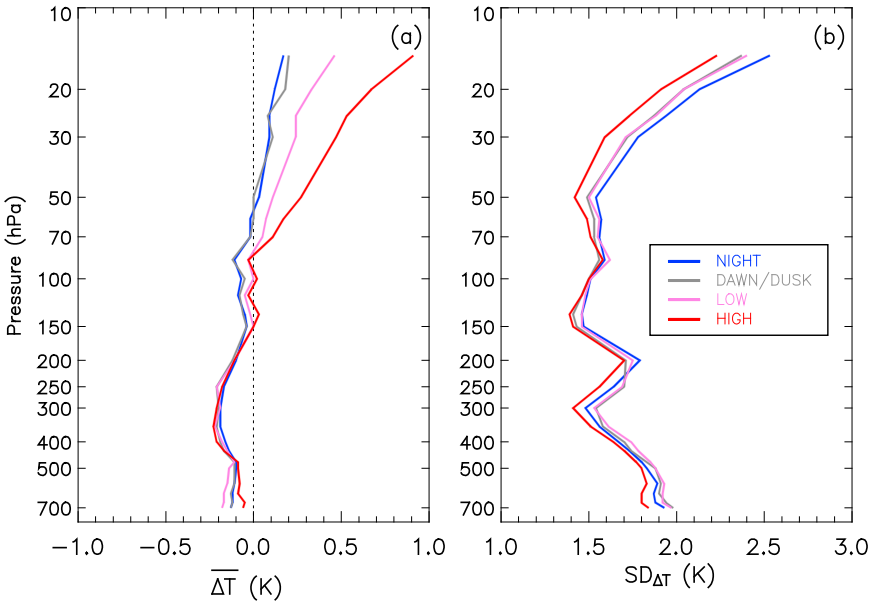

Figure 3. Vaisala RS92 RAOB-minus-COSMIC (a) mean temperature difference and (b) its standard deviation based on its global collocation data for May 2008 to August 2011. The curves in different colors show results segregated by solar elevation angle class.

080), and Autosonde (code 081). These codes refer to different ground stations, not different radiosondes, and these subtypes use the same radiation corrections, but the specific correction version used at each station is rarely documented. As expected, the biases are similar for all three types for daytime SEA classes (not shown). But, for NIGHT, $\overline{\Delta T}$ for DigiCora I, II, or Marwin is 0.26 K, while it is only 0.04 K and 0.08 K for DigiCora III and Autosonde, respectively. All three types are used widely, but DigiCora I, II, or Marwin tends to be more widely used in low latitudes or regions of warmer climates, indicating again

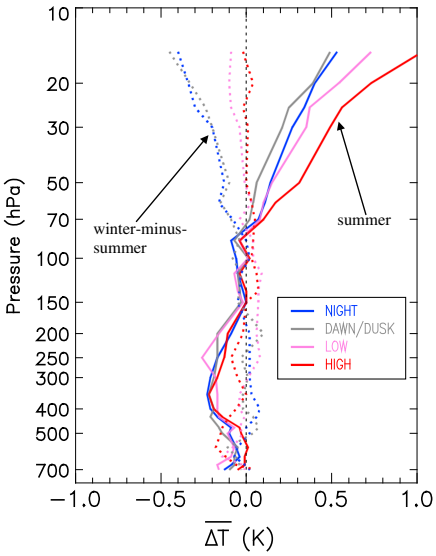

Figure 4. Vaisala RS92 RAOB-minus-COSMIC mean temperature differences for Northern Hemisphere summer (solid curves) and winter-minus-summer differences (dashed curves).

a warmer nighttime $\overline{\Delta T}$ is associated with a warmer climate regime.

[26] Older white-painted rod thermistors have significant infrared cooling at night [*Luers and Eskridge*, 1995]. The Vaisala RS92 temperature sensor (F-Thermocap, also used in Vaisala RS90 [*Miloshevich et al.*, 2006]), a very thin silver-coated wire, is expected to be insensitive to environmental temperature changes if other radiative parameters remain the same, such as SEA and cloud cover.

[27] In a warm climate, temperature typically rises faster with altitude in the stratosphere than in a cold climate. If sensor time lag error is a possible explanation for the seasonal or regional bias variations, it, if present, should cause the bias to be more negative in the warm climate, which is opposite to what we noticed in the data. Furthermore, *Luers* [1997] pointed out the time lag error for the F-Thermocap sensor is insignificant due to the small size of this sensor plus its low emissivity of the aluminum coating. In summary, it remains unclear why the Vaisala RS92 nighttime $\overline{\Delta T}$ varies with climate regimes.

[28] *MRZ*. The Russian Federation upper air network includes ~124 stations including 2 stations in Antarctica. They used MARS (codes 028 and 029, phased out during this period) and MRZ (codes 027, 075, and 088 with different ground stations) sondes, introduced in the mid-1980s. All these models use an MMT-1 rod thermistor and a goldbeater's skin humidity sensor. MRZ-3A* or MRZ* (previously called BAR), code 058 or 089, is being phased in and has the same rod thermistor but a different humidity sensor. Here, we use only data from codes 027, 058, 075, 088, and 089.

[29] As shown in Figure 5, these sondes show a strong warm bias above 200 hPa for daytime SEAs, with bias larger for HIGH and LOW than for DUSK/DAWN. Unique among the sonde types analyzed in this study, the Russian sonde biases are almost constant with height above 150 hPa. A

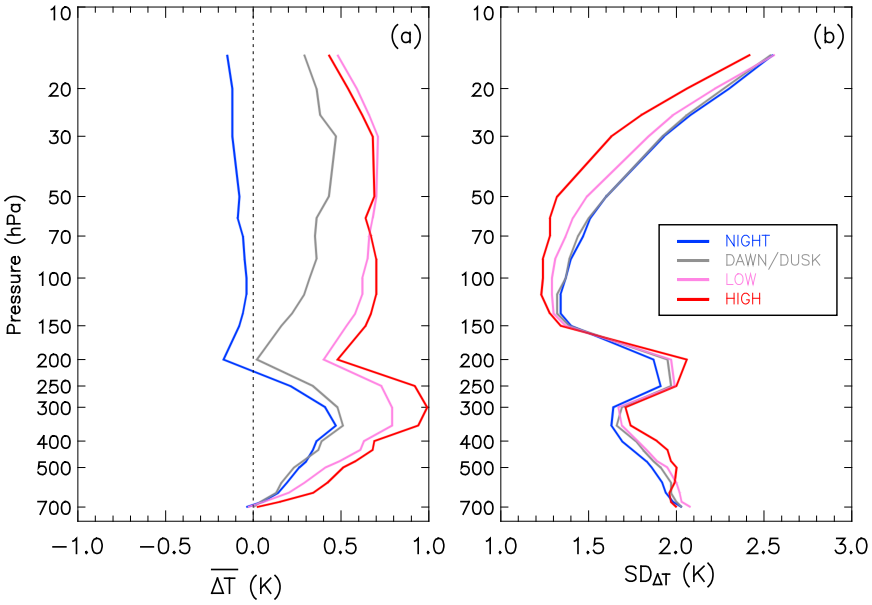

Figure 5. Same as Figure 3 except for Russian MRZ.

cold bias at night increases slightly with altitude, reaching ~0.15 K at 15 hPa.

[30] Another unique feature is a strong warm bias in the middle and upper troposphere. These Russian sondes account for ~22% of total global reports and so contribute significantly to the warm tropospheric bias shown in Figure 10 for the "older" sondes. Different from Vaisala RS92 and other types, the MRZ temperature in the middle and upper troposphere is warmer (by ~0.23 K) than GFS forecast with the latter agreeing with COSMIC within 0.1 K, suggesting that MRZ measurements might be ignored in the NCEP NWP assimilation.

[31] *Sippican-B2*. This sonde was introduced at many U.S. upper air sites in 1997, but by 2012, only Caribou, Guam, five Alaskan, and eight Caribbean sites used this radiosonde. The Sippican-B2 thermistor is a long white-coated rod, and it is expected to have a very large infrared error.

[32] The Sippican-B2 profiles (Figure 6) reveal nighttime cold biases and daytime warm biases. The NIGHT bias increases with altitude, from 0.2 K at 700 hPa to 1.7 K at 15 hPa. Daytime biases are small (< 0.35 K) at 15–70 hPa for LOW and DUSK/DAWN; for class HIGH, the bias is much larger (1.38 K). A strong regional variation is noted for NIGHT. For example, the 15–150 hPa NIGHT bias for stations in Alaska reaches −1.48 K but is 0.35 K for tropical stations.

[33] *Sippican Mark IIA*. The NWS currently uses mainly Sippican Mark IIA GPS radiosondes (code 087) with a chip thermistor, for which no corrections are applied for infrared effects [*Fitzgibbon and Facundo*, 2003]. A systematic cold

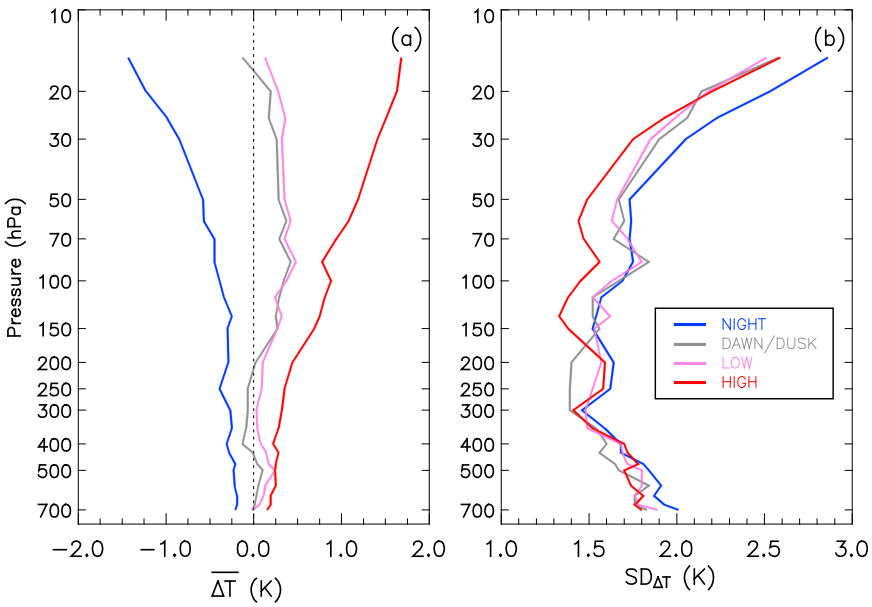

Figure 6. Same as Figure 3 except for Sippican-B2.

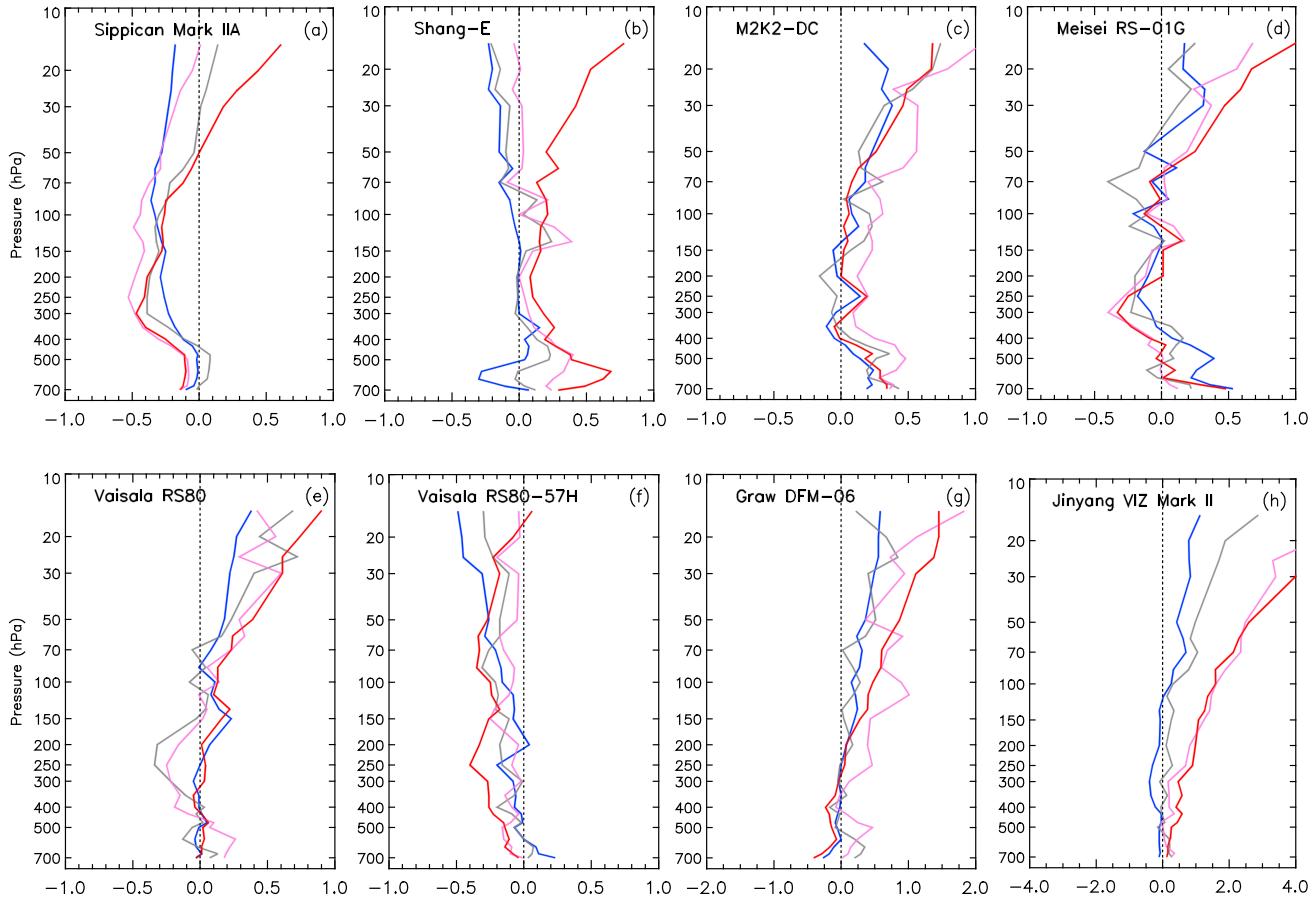

Figure 7. Same as Figure 3a except for other sonde types.

bias is shown (Figure 7a) for all SEA classes except HIGH in Sippican Mark IIA for the middle troposphere to ~100 hPa, which gradually decreases toward the stratosphere. For class HIGH, a warm bias is found from 50 to 15 hPa.

[34] *Shang-E*. In China, starting January 2002, the digital Shang-E with a rod thermistor and a carbon hygristor was introduced into the radiosonde network to replace the Shang-M with a bimetal coil temperature sensor and a goldbeater's skin humidity sensor. Chinese stations started reporting 31313 instrument codes starting in October 2012, and about 80% of the stations used Shanghai GTS1 with nearly equal numbers of the other stations reporting Taiyuan GTS1-1 and Nanjing GTS1-2, but it is unknown if each station used the same variety back to 2008. In this work, we exclude data from seven stations that flew Shang-M (which was identified by persistently higher reported relative humidity than any of the Shang-E models) during the study period and average data only for Shang-E sondes (but not differentiating its different models) to compute the bias statistics.

[35] In general, the Chinese sonde bias is < 0.2 K except for HIGH SEA when the warm bias at altitudes above 70 hPa exceeds 0.5 K (Figure 7b). Note that only 5.6% of the total profiles are in the HIGH SEA class.

[36] *M2K2-DC*. The Modem M2K2-DC (code 057) is widely used in France and French ships, French-speaking countries in Africa and Oceania, Iran, India, Malaysia, and a few other countries. There are systematic warm biases above the tropopause that increase with heights for all SEA classes (Figure 7c). The NIGHT warm bias is smaller than those of other SEA classes, but overall, the biases do not distinguish among classes perhaps because the profile sample is not big enough.

[37] *Meisei RS-01G*. Most stations on Japanese islands have been frequently using Vaisala RS92 starting 2008. Meisei RS-01G sondes (code 055) are used primarily over western tropical Pacific islands. The sample for this instrument is only 1194 but distributes relatively evenly among the SEA classes. As shown in Figure 7d, temperature measurements from this instrument are reasonably consistent with COSMIC data for altitudes between 70 and 150 hPa. But, above 70 hPa, Meisei RS-01G shows warm biases that increase with height for all SEAs. The instrument biases found here are similar to those from the 2011 Yangjiang radiosonde intercomparison experiment [*Nash et al.*, 2011].

[38] *Vaisala RS80*. This is the sonde type NCEP used as the reference to develop radiation correction for other sonde types (http://www.emc.ncep.noaa.gov/mmb/papers/collins/new_tables/new_tables.html) in the late 1990s when the Vaisala RS80 was the most widely used advanced sonde.

[39] The radiosonde temperature for SEA class ALL (not shown) matches well with COSMIC data in the troposphere below 200 hPa. Warm biases are exhibited starting ~100 hPa that increase with height and SEA (Figure 7e).

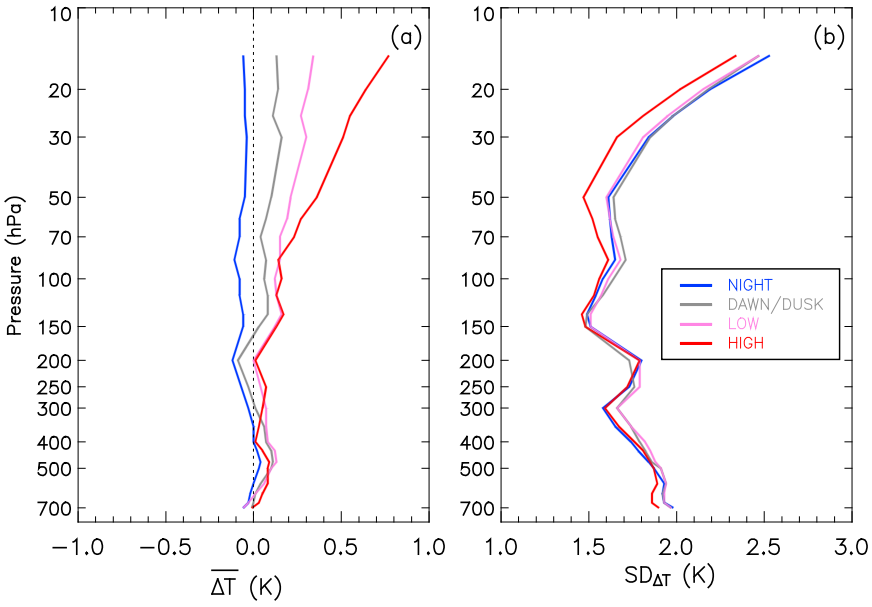

Figure 8. Same as Figure 3 except for global data.

[40] *Vaisala RS80-57H*. This sonde was the U.S. NWS Vaisala RS80 version used starting June 1998 at almost all U.S. stations not using Sippican-B2 but phased out after December 2010. Since 2008, only a few stations in Alaska and the Pacific and some stations in southern Africa have used this sonde. Vaisala RS80-57H used standard RS80 sensors, but their data processing procedures differed because RS80-57H operated with NWS instead of Vaisala ground systems [*Redder et al*., 2004].

[41] The $\overline{\Delta T}$ profiles for different SEAs are intertwined, but they all show a cold bias that increases with height starting at the low troposphere (Figure 7f). It is uncertain if the bias is related to the error in the U.S. RS80/RSN93 correction software found from WMO intercomparison data noted by *Redder et al*. [2004].

[42] *Graw DFM-06*. This sonde (reporting code 017 instead of 018) is mainly used in Germany, NATO military units, Denmark, Turkey, India, and several other countries. Warm biases are shown in Figure 7g starting in the upper troposphere and increasing with altitude toward the low stratosphere for both daytime and NIGHT SEAs as well. This feature is somewhat consistent with the results from the 2010 Yangjiang intercomparison experiment [*Nash et al*., 2011] that Graw biases show a positive shift in temperature relative to other radiosonde systems when passing the tropopause and these shifts occur in both day and night measurements. Similar bias characteristics were also noticed in Graw DFM-97 in the WMO radiosonde intercomparisons conducted at Vacoas, Mauritius, on 7–27 February 2005 [*Nash et al*., 2006].

[43] *Jinyang*. Only three stations in South Korea are flying Jinyang radiosondes (code 21). While code 21 is assigned to Jinyang VIZ Mark II, the same code is probably used to indicate Jinyang RSG-20A, the current radiosonde, which was also used in the 2010 Yangjiang intercomparison [*Nash et al*., 2011]. As displayed in Figure 7h, warm biases are shown in the data with greater biases at higher SEA classes.

[44] The bias for this sonde is the greatest among the types analyzed. But, it showed a slight cold bias for both night and day compared to other sondes in the Yangjiang radiosonde experiment [*Nash et al*., 2011], where a radiation correction was implemented. Obviously, that correction worked effectively to remove radiation biases shown in Figure 7h.

[45] *Vaisala RS90*. This sonde, carrying sensors equivalent to Vaisala RS92 in terms of calibration accuracy and time response [*Miloshevich et al*., 2006], has been gradually phased out, and the sample number for the period studied is far less than that of Vaisala RS92, but they show similar biases. The bias pattern plot is not given for this sonde in Figure 7.

[46] *IMD Mark IV*. Measurements from most of the Indian stations flying IMD Mark IV are limited to below 100 hPa. For this analysis, data from only the stations flying that sonde were used, and a cold bias of 0.3 K is noticed for NIGHT and DAWN/DUSK between 200 and 300 hPa and a warm bias is then shown for all SEA classes at 100–150 hPa (the bias plot for this sonde is not shown in Figure 7). For this sonde, the $SD_{\Delta T}$ shows a strong increase with height from the low to the upper troposphere, which is not seen in other sonde types.

3.2. Global Bias Pattern

[47] Figure 8 shows $\overline{\Delta T}$ and $SD_{\Delta T}$ computed using all ~187,000 global collocations for each SEA class (the actual sample size for 15–70 hPa for global data is ~145,000; see Table 3). There are small (< 0.1 K) nighttime cold biases that do not vary with altitude and larger daytime warm biases that are larger above 200 hPa than below and that increase with increasing SEA. The daytime mean bias at 15 hPa for SEA $> 22.5°$ reaches 0.77 ± 2.34 K. Note the "global" bias statistics shown in Figure 8 were computed by simply combining sounding data from all sonde types available, not weighted by their area coverage, and the same is true for other statistics computed from the mixture of sonde types.

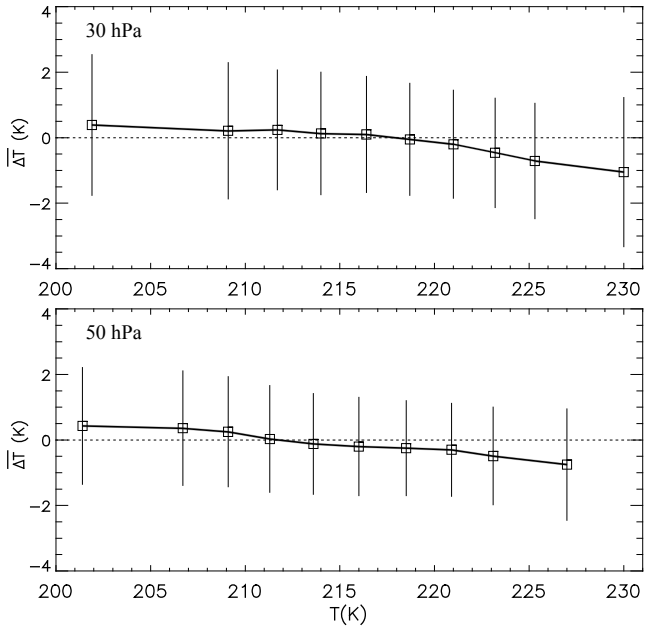

Figure 9. Variation of night RAOB-minus-COSMIC mean temperature difference with temperature based on global collocation data during May 2008 to October 2011 at 30 hPa and 50 hPa. The vertical lines are one standard deviation difference (K). Except for the leftmost (rightmost) values on the *x* axis which are averaged from temperatures less (greater) than the specified values, other temperature values are averaged in 2.5 K bins, based on COSMIC dry temperature.

[48] Although the NIGHT cold bias computed from global data is small, it varies with ambient temperature (Figure 9). At the lowest T (< 210 K), the bias is positive (warm bias), but for $T > 215$ K, the cold bias increases with increasing T. We find similar features for individual operational sondes, for example, in Russian MRZ and Vaisala RS92, consistent with radiosonde intercomparison experiments (See document available at http://www.wmo.int/pages/prog/www/IMOP/meetings/Upper-Air/Systems-Intercomp/DocPlan.html). Potential explanations for this pattern include the following: (1) uncorrected time lag in the stratosphere where T generally increases with height and (2) infrared radiative cooling by high level clouds as discussed in section 3.2.3.

3.2.1. Older Versus Newer Sondes

[49] To improve upon temperature corrections applied at stations (or to correct uncorrected data), NCEP applies additional radiation corrections (http://www.emc.ncep.noaa.gov/mmb/papers/collins/new_tables/new_tables.html)

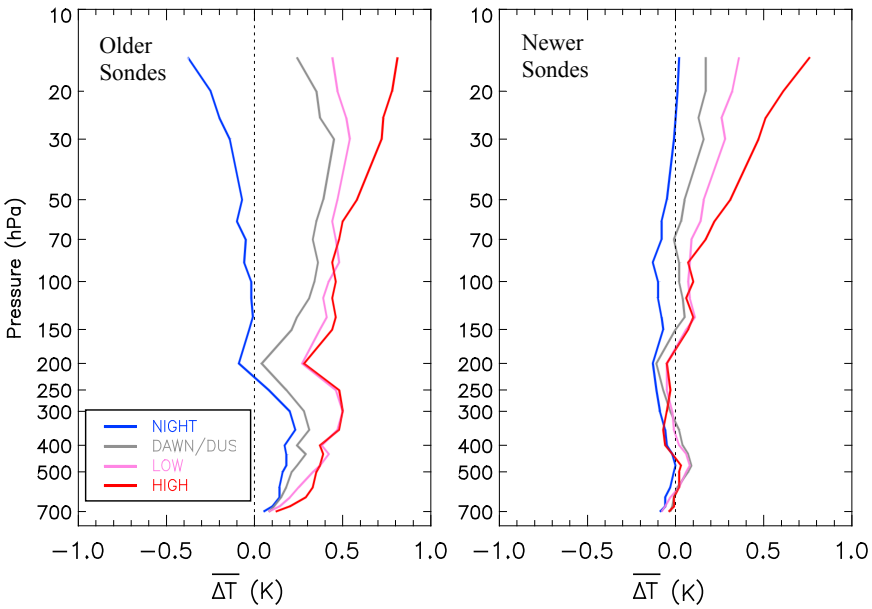

Figure 10. Same as Figure 3a except for older and newer sonde types.

Table 2a. RAOB-Minus-COSMIC Mean Differences (K) and Standard Deviations (K) for Different Latitude Bands and Solar Elevation Angles Over 15–70 hPa[a]

	NIGHT	DUSK/DAWN	LOW	HIGH	ALL
Tropic (10°S–10°N)	0.36 (2.01, 919)	0.38 (2.05, 843)	0.42 (2.04, 709)	0.31 (2.01, 1055)	0.36 (2.02, 3526)
Subtropic (10°N–30°N)	0.20 (1.96, 4561)	0.03 (2.06, 3478)	0.20 (2.04, 2191)	0.68 (1.94, 3023)	0.26 (2.01, 13,253)
Midlatitude (30°N–50°N)	−0.03 (1.86, 22,857)	0.06 (1.91, 10,256)	0.14 (1.94, 9512)	0.49 (1.80, 14,477)	0.15 (1.88, 57,102)
High latitude (> 50°N)	−0.20 (1.89, 20,076)	0.15 (1.82, 12,130)	0.34 (1.76, 11,949)	0.45 (1.58, 14,170)	0.15 (1.80, 58,325)

[a]Values in parentheses are standard deviation and sample size.

that depend on sonde type, height, and SEA. However, they have not been updated since around 2000, and NCEP currently applies no correction to newer sondes. To evaluate the potential need to update NCEP's correction scheme, we compare the biases of "older" and "newer" sondes, where "older" sondes are defined as ones to which NCEP applies corrections (including Vaisala RS80, RS80-57H, and RS90; Sippican-B2; and Russian MRZ) while "newer" sondes are those introduced since around 2000 (including Vaisala RS92, Sippican Mark IIA, and Chinese Shang-E). All comparisons use radiosonde data without NCEP corrections. The sample sizes are 33,516 soundings from older sondes and 153,565 newer sondes.

[50] Both older and newer sondes show nighttime cold biases and daytime warm biases, the latter increasing with altitude and SEA (Figure 10). But, newer sondes have smaller biases. For example, above 150 hPa, the average NIGHT biases are -0.05 ± 1.78 K for newer sondes and -0.12 ± 1.81 K for older sondes; at LOW SEA, newer and older sonde biases are 0.19 ± 1.76 K and 0.47 ± 1.82 K, respectively. The differences in bias between the older and newer sondes for these two SEA classes are statistically significant at the 0.05 or better level.

3.2.2. Latitudinal and Seasonal Variability

[51] Collocations south of 10°S are included in global analyses above but are not numerous enough to be analyzed here by latitude belts. Table 2a gives $\overline{\Delta T}$ averaged over 15–70 hPa in four different zonal bands that span the region from 10°S to 90°N, in each SEA class. All latitudinal bands show a warm bias for class ALL, and the bias increases from high to low latitudes. Daytime warm biases increase with SEA, except in tropics, where the $\overline{\Delta T}$ dependence on SEA is smaller than that in other zones and where the bias for class HIGH is less than that for LOW by (statistically insignificant) 0.11 K. For NIGHT, a slight cold bias is found at middle and high latitudes, which is significantly different from the warm biases of 0.20 K and 0.36 K in subtropics and tropics, respectively.

[52] Table 2b shows $\overline{\Delta T}$ collocations north of 20°N for each season and SEA class. All seasons show a warm bias for class ALL, the largest in summer (0.28 K) and the smallest in winter (0.08 K). In all seasons, the daytime bias increases from DUSK/DAWN to LOW and to HIGH SEA. For NIGHT, $\overline{\Delta T}$ is negative (0.06 K–0.16 K), except in summer which shows a significantly different warm bias of 0.14 K.

[53] The latitudinal or seasonal dependence of biases, particularly for NIGHT, for individual sonde types (including Vaisala RS92 and Sippican-B2; see section 3.1) is qualitatively consistent with what we obtain using the data of all sonde types listed in Tables 2a and 2b. For NIGHT, the zonal and seasonal analysis suggests a sonde warm bias is associated with warm climate conditions (summer, tropics) and a less warm or cold bias is associated with cold climate conditions. Some old temperature sensors using large white-coated rod thermistors absorb longwave energy emitted from the surface or atmosphere [*Luers and Eskridge*, 1995, 1998; *McMillin et al*., 1992] and so have a warm bias in warm conditions. But, newer sondes, including Vaisala RS92, also have nighttime warm biases, as was discussed in section 3.1, and a ready explanation is not obvious.

3.2.3. Cloud Effects

[54] Clouds reflect and scatter solar radiation and emit infrared radiation that can affect the radiative energy balance surrounding radiosonde sensors. Different cloud types have different radiative impacts. In general, these cloud effects are not considered in radiation correction schemes for operational sondes. The exception is the Mark IIA, for which reported cloud group is used to correct measurements [*Bower and Fitzgibbon*, 2004].

[55] Cloud information reported at radiosonde sites includes low or middle level cloud cover, low cloud type, height of low or middle cloud base, and middle and high level cloud types. Some sites do not report clouds, including those in Finland, Sweden, Iceland, South Korea, Japan, China, Canada, USA (military sites), Mexico, Venezuela, and Australia. We therefore use reports from other countries/regions, which account for ~48% of the global observations, to estimate the effect of cloud presence on radiosonde radiation biases.

Table 2b. Global RAOB-Minus-COSMIC Mean Differences (K) and Standard Deviations (K) for Different Seasons and Solar Elevation Angles Averaged Over 15–70 hPa From Data of Northern Hemisphere North of 20°N[a]

	NIGHT	DUSK/DAWN	LOW	HIGH	ALL
Winter	−0.11 (2.16, 15,186)	0.10 (2.20, 5865)	0.28 (2.16, 5815)	0.55 (1.97, 3572)	0.08 (2.16, 30,438)
Spring	−0.16 (1.78, 13,261)	0.05 (1.83, 7206)	0.20 (1.81, 6335)	0.47 (1.75, 10,856)	0.12 (1.81, 37,658)
Summer	0.14 (1.70, 9848)	0.13 (1.75, 9036)	0.26 (1.69, 8254)	0.47 (1.66, 15,060)	0.28 (1.70, 42,198)
Autumn	−0.06 (1.78, 11,739)	0.16 (1.86, 5589)	0.28 (1.86, 5593)	0.51 (1.72, 5774)	0.16 (1.81, 28,695)

[a]Winter is December-January-February, etc. Values in parentheses are standard deviation and sample size.

Table 2c. RAOB-Minus-COSMIC Mean Biases (K) and Standard Deviations (K) for Different Cloud Sky Conditions and Solar Elevation Angles Averaged Over 15–70 hPa[a]

	NIGHT	DUSK/DAWN	LOW	HIGH	ALL
Clear	0.03 (1.81, 9745)	0.33 (1.93, 2304)	0.41 (1.90, 1895)	0.64 (1.77, 3050)	0.22 (1.85, 16,994)
Cloudy	−0.02 (1.89, 15,433)	0.23 (1.88, 9898)	0.34 (1.88, 9862)	0.46 (1.73, 17,902)	0.25 (1.84, 53,095)

[a]The statistics were computed from countries/regions where cloud information is included in radiosonde reports (see text for detail). Values in parentheses are standard deviation and sample size.

[56] We first examine $\overline{\Delta T}$ for clear and cloudy sky conditions. Clear sky is defined as no cloud present at low, middle, and high levels and cloudy as cloud present at least one of the three levels. Our results (Table 2c) indicate that for nighttime, there are a slight cold bias in cloudy sky conditions and a slight warm bias for clear sky. For daytime, both sky condition categories show a warm bias that increases with altitude (figure not shown) and with SEA in the upper troposphere and low stratosphere. However, the warm bias is larger in clear skies than for cloudy conditions particularly for the HIGH class for which their bias difference is 0.18 K, statistically significant at better than the 0.05 level. The statistics in Table 2c were computed using data from both older and newer sondes, as defined in section 3.2.1. We did a similar analysis but for newer sondes, which account for 78% of all profiles used in Table 2c. In general, newer sonde types have lower biases in all cloud categories than those in Table 2c. For example, the $\overline{\Delta T}$ values for 15–70 hPa are 0.27 ± 1.87 K and 0.44 ± 1.73 K for the LOW and HIGH classes, respectively. The climatological biases may reflect the overall effect of clouds, including their type, height, amount, and thickness and the location of the sonde (i.e., below cloud deck or above cloud top; see *Bower and Fitzgibbon* [2004] and *McMillin et al.* [1992]), and they suggest that clouds can reduce the solar radiation impacts on sensor temperature.

[57] High clouds, which are generally cirrus clouds, are colder than the surrounding environment and so cause an infrared cooling of surrounding air. We examine the $\overline{\Delta T}$ values separately for high level clouds and low or middle level clouds. For nighttime, there is a 0.05 K cold bias in high cloud conditions, while the bias is close to zero when only low or middle level clouds are reported. For daytime, the warm biases in high cloud conditions are less than those in low or middle cloud conditions, for example, their difference being −0.12 K, statistically significant for the HIGH class. Cooling from water or ice coating on the sensor as it passes through a cloud, generally stronger for high clouds than for low or middle clouds, can contribute to those bias differences. Restricting this analysis to newer sondes, we found again biases are reduced for these two sky conditions compared with all sondes.

4. Radiation Errors in RAOBs, NWP Forecast, and COSMIC Retrievals

[58] Along with satellite and other in situ data, RAOBs are assimilated in the NWP system to generate a forecast [*Ballish and Kumar*, 2008], and the forecast is then used for many applications, including, pertinent to this work, as the first guess in COSMIC wet retrievals. A comparison of the first-guess NCEP GFS forecast data with COSMIC T_d may determine if the radiosonde radiation-induced biases discussed in section 3 influence the forecast data. Figure 11 indicates that there is a signature of the radiosonde warm biases in the low stratosphere in the GFS forecast, even though the GFS warm biases are largely reduced relative to RAOBs, likely due to the assimilation of satellite radiance data, which do not contain such biases.

[59] A similar analysis was also done for COSMIC T_w for which the biases are smaller than its first guess in all daytime SEA classes (Figure 11), suggesting that COSMIC T_w profiles from 1DVar show improvement over its first guess but still retain warm bias components in the upper troposphere and low stratosphere via the initial NWP assimilation of "warm" RAOBs. Figure 11 emphasizes the importance of eliminating radiosonde radiation biases in NWP assimilation.

5. Conclusion and Discussion

[60] Using COSMIC GPSRO as a reference, this study has quantified temperature biases in radiosonde observations, with a focus on the upper troposphere and low stratosphere where radiation-induced errors are greatest. Overall, the global radiosonde network has a nighttime cold bias and a

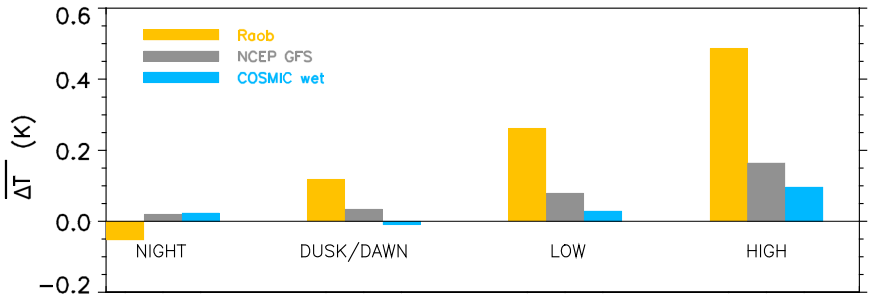

Figure 11. Mean RAOB, NCEP GFS, and COSMIC wet retrieval temperature differences from COSMIC dry temperature at 15–70 hPa for different solar elevation angle categories.

Table 3. RAOB-Minus-COSMIC Mean Biases (K) and Standard Deviation Differences (K) for Different Sonde Types and Solar Elevation Angles Averaged Over 15–70 hPa[a]

Type	NIGHT	DUSK/DAWN	LOW	HIGH	ALL
RS80	0.22 (1.82, 1162)	0.39 (1.77, 88)	0.42 (1.98, 198)	0.55 (1.78, 960)	0.37 (1.83, 2408)
RS80-57H	−0.35 (1.80, 1293)	−0.20 (1.76, 418)	*−0.08* (1.79, 420)	−0.19 (1.57, 974)	−0.24 (1.73, 3105)
RS90	*0.06* (1.70, 1029)	*0.07* (1.54, 302)	*0.02* (1.55, 547)	0.35 (1.66, 866)	0.15 (1.65, 2744)
RS92	0.07 (1.84, 19,719)	0.08 (1.77, 8507)	0.22 (1.78, 9955)	0.46 (1.67, 15,926)	0.21 (1.78, 54,107)
M2K2-DC	0.28 (1.88, 948)	0.38 (2.11, 290)	0.59 (2.02, 315)	0.42 (1.81, 1074)	0.38 (1.90, 2627)
DFM-06	0.45 (1.88, 651)	0.49 (2.12, 69)	0.88 (2.21, 31)	1.11 (2.13, 445)	0.71 (2.03, 1196)
RS-01G	*0.14* (1.87, 323)	*0.02* (1.78, 204)	0.32 (1.76, 166)	0.45 (1.64, 271)	0.23 (1.78, 964)
Sippican-B2	−0.87 (2.11, 1685)	0.22 (1.94, 996)	0.32 (1.91, 789)	1.38 (1.82, 1133)	0.12 (2.16, 4603)
Sippican Mark IIA	−0.25 (1.78, 7836)	*0.00* (1.81, 3787)	−0.18 (1.83, 3559)	0.19 (1.68, 5075)	−0.08 (1.78, 20,257)
Shang-E	−0.16 (2.05, 2721)	−0.12 (2.01, 4935)	*0.00* (1.91, 2660)	0.40 (1.81, 615)	−0.07 (1.99, 10,931)
Jinyang	0.72 (2.21, 240)	1.50 (2.30, 67)	3.30 (2.08, 63)	3.65 (2.08, 188)	2.12 (2.57, 558)
MRZ	−0.11 (1.93, 10,598)	0.40 (1.91, 6935)	0.66 (1.84, 6531)	0.62 (1.67, 7462)	0.34 (1.88, 31,526)
All types	−0.05 (1.89, 51,827)	0.12 (1.90, 28,913)	0.26 (1.87, 27,191)	0.49 (1.74, 37,274)	0.18 (1.86, 145,205)

[a]Values inside the parentheses are standard deviation and sample size. All the biases are statistically significant at the 0.05 or better level except the italicized ones.

daytime warm bias with daytime bias increasing with altitude and solar elevation angle. Daytime warm biases associated with clouds are smaller than those in clear conditions. Newer sondes (introduced after 2000) have smaller biases than older sondes and appear to be less influenced by cloud effects, perhaps due to the improved sensor technology. Biases at night show greater seasonal and zonal variations than those for daytime. In general, warm NIGHT biases are associated with warm climate regimes, and less warm or cold biases are associated with cold climate regimes. Temperature biases vary among sonde types (Table 3): The results for 13 types, accounting for 92% of the global network, are presented for eventual incorporation in new corrections to radiosonde temperature data in numerical weather prediction, satellite calibration and validation, and climate research applications.

[61] The radiosonde biases in the low stratosphere revealed in this analysis appear to be greater than those found in the most recent WMO Intercomparison of High Quality Radiosonde Systems in Yangjiang, China, in July 2010 [*Nash et al*., 2011]. That intercomparison used a combination of multiple sensors as a reference for comparison, so a bias in any of the sensors may well be related to the bias in the reference. Because it was a special field experiment, radiation correction schemes used in the 2010 intercomparison may be more advanced than the ones used in the operational network (for example, the 2010 correction version was used for Vaisala RS92 in the 2010 intercomparison while the 2005 version for operational ones), and some manufacturers tuned their radiation corrections to match that of Vaisala (H. Vömel, personal communication, 2012) in the 2010 intercomparison. All these factors can reduce the biases for individual sonde types intercompared in the 2010 experiment. Our analysis using COSMIC as a reference provides a clearer indication of biases in different sonde types. Moreover, our analysis is not limited to a single location and a short test period.

[62] As shown in Table 3, not all radiosondes have warm "daytime" biases and cold "nighttime" biases. Errors other than radiation-induced ones, such as calibration error, time lag error, or errors in data processing, could be responsible for those biases for some sonde types. Also, temperature measurements for some sonde types might be overcorrected (undercorrected) by their existing schemes, e.g., corrections that are too large could result in a cold daytime bias and a warm night bias while corrections that are too small could cause a warm daytime bias and a cold night bias.

[63] The statistics in this analysis were computed from ~3 year RAOB-COSMIC collocations. More data are needed to obtain statistically more robust bias characteristics for sonde types particularly the minor ones. Also, the RAOB and COSMIC collocations are not perfectly collocated. GPSRO and radiosonde profiles differ in several ways in terms of measurement characteristics, including profile geometry and horizontal resolution. A radiosonde makes point measurements but balloon drifts an average of ~50 km horizontally during the ~100 min ascent from the surface to the stratosphere [*Seidel et al*., 2011]. Although GPSRO profiles have fine vertical resolution (0.5 km in the low troposphere and 1.5 km in the middle atmosphere) by satellite retrieval standards, they have a wide horizontal resolution, ranging from ~160 km at the low troposphere to 320 km in the upper atmosphere (i.e., ~250 km, defined by the distance traversed by the radio path as it enters and exits a layer [*Kursinski et al*., 1997]). Future research is needed to understand the impacts of those differences on a data comparison analysis like this.

[64] **Acknowledgments.** The authors thank Anthony Mannucci and Chi Ao for the helpful discussions on COSMIC data, Holger Vömel and Carl Bower for the information on radiosonde instrument characteristics, Michael Hicks and John Kochendorfer for the comments on the manuscript, Frank Tilley and Michael Pettey for some data processing, and the three anonymous reviewers for their constructive suggestions for improving this paper.

References

Anthes, R. A., et al. (2008), The COSMIC/FORMOSAT-3 mission: Early results, *Bull. Amer. Meteor. Soc.*, *89*, 313–333.

Ao, C. O. (2007), Effect of ducting on radio occultation measurements: An assessment based on high-resolution radiosonde soundings, *Radio Sci.*, *42*, RS2008, doi:10.1029/2006RS003485.

Ballish, B. A., and V. K. Kumar (2008), Systematic differences in aircraft and radiosonde temperatures: Implications for NWP and climate studies, *Bull. Amer. Meteor. Soc.*, *89*, 689–707, doi:10.1175/2008BAMS2332.1.

Bower, C. A., and J. J. Fitzgibbon (2004), National Weather Service in-situ radiation temperature correction for Radiosonde Replacement System GPS radiosondes. Eighth Symposium on Integrated Observing and Assimilation Systems for Atmosphere, Oceans, and Land Surface. The 84th American Meteorological Society Annual Meeting, Seattle, WA, 10–16 January 2004 (available online at http://ams.confex.com/ams/pdfpapers/74046.pdf).

Bower, C. A., and J. J. Fitzgibbon (2003), Flight temperature comparisons between the NASA Three Thermistor Reference radiosonde and the National Weather Service qualified GPS radiosondes. 12th Symposium on Meteorological Observations and Instrumentation, the 83rd American Meteorological Annual Meeting, Long Beach, CA, 9–14 February 2003 (available online at http://ams.confex.com/ams/pdfpapers/51582.pdf).

Christy, J. R., and W. B. Norris (2009), Discontinuity issues with radiosonde and satellite temperatures in the Australian region 1979–2006, *J. Atmos. Ocean. Tech.*, *26*, 508–522.

Collins, W. G. (2001a), The operational complex quality control of radiosonde heights and temperatures at the National Centers for Environmental Prediction. Part I: Description of the method, *J. Appl. Meteor.*, *40*, 137–151.

Collins, W. G. (2001b), The operational complex quality control of radiosonde heights and temperatures at the National Centers for Environmental Prediction. Part II: Examples of error diagnosis and correction from operational use, *J. Appl. Meteor.*, *40*, 152–168.

Redder, C. R., J. K. Luers, and R. E. Eskridge (2004), Unexplained discontinuity in the U.S. radiosonde temperature data. Part II: Stratosphere, *J. Atmos. Ocean. Tech.*, *21*, 1133–1144.

Fitzgibbon, J. J., and J. Facundo (2003), Developing a technique for verifying radiosonde solar radiation correction algorithms. American Meteorological Society [available online at http://ams.confex.com/ams/pdfpapers/54317.pdf].

Free, M., J. K. Angle, I. Durre, J. Lanzante, T. C. Peterson, and D. J. Seidel (2004), Using first differences to reduce inhomogeneity in radiosonde temperature datasets, *J. Clim.*, *17*, 4171–4179.

Gaffen, D. J. (1994), Temporal inhomogeneities in radiosonde temperature records, *J. Geophys. Res.*, *99* (D2), 3667–3676.

Haimberger L., C. Tavolato, and S. Sperka (2008), Toward elimination of the warm bias in historic radiosonde temperature records—Some new results from a comprehensive intercomparison of upper-air data, *J. Clim.*, *21*, 4587–4606.

Hajj, G. A., E. R. Kursinski, L. J. Romans, W. I. Bertiger, and S. S. Leroy (2002), A technical description of atmospheric sounding by GPS occultation, *J. Atmos. Solar-Terrestrial Physic.*, *64*, 451–469.

Hajj, G. A., C. O. Ao, B. A. Iijima, D. Kuang, E. R. Kursinski, A. J. Mannucci, T. K. Meehan, L. J. Romans, M. de la Torre Juarez, and T. P. Yunck (2004), CHAMP and SAC-C atmospheric occultation results and intercomparisons, *J. Geophys. Res.*, *109*, D06109, doi:10.1029/2003JD003909.

He, W., S.-P. Ho, H. Chen, X. Zhou, D. Hunt, and Y.-H. Kuo (2009), Assessment of radiosonde temperature measurements in the upper troposphere and lower stratosphere using COSMIC radio occultation data, *Geophys. Res. Lett.*, *36*, L17807, doi:10.1029/2009GL038712.

Ho, S.-P., Y.-H. Kuo, Z. Zeng, and T. C. Peterson (2007), A comparison of lower stratosphere temperature from microwave measurements with CHAMP GPS RO data, *Geophys. Res. Lett.*, *34*, L15701, doi:10.1029/2007GL030202.

Ho, S.-P., et al. (2012): Reproducibility of GPS radio occultation data for climate monitoring: Profile-to-profile inter-comparison of CHAMP climate records 2002 to 2008 from six data centers, *J. Geophys. Res.*, *117*, D18111, doi:10.1029/2012JD017665.

Kuo, Y.-H., W. S. Schreiner, J. Wang, D. L. Rossiter, and Y. Zhang (2005), Comparison of GPS radio occultation soundings with radiosondes, *Geophys. Res. Lett.*, *32*, L05817, doi:10.1029/2004GL021443.

Kursinski, E. R., G. A. Hajj, J. T. Schofield, R. P. Linfield, and K. R. Hardy (1997), Observing Earth's atmosphere with radio occultation measurements using the Global Positioning System, *J. Geophys. Res.*, *102*, (D19), 23,429–23,465.

Lanzante, J. R., S. A. Klein, and D. J. Seidel (2003), Temporal homogeneization of monthly radiosonde temperature data. Part I: Methodology, *J. Clim.*, *16*, 224–240.

Luers, J. K., and R. E. Eskridge (1998), Use of radiosonde temperature data in climate studies, *J. Clim.*, *11*, 1002–1019.

Luers, J. K., 1997: Temperature error of the Vaisala RS90 radiosonde, *J. Atmos. Oceanic Tech.*, *14*, 1520–1532.

Luers, J. K., and R. E. Eskridge (1995), Temperature corrections for the VIZ and Vaisala radiosondes, *J. Appl. Meteor.*, *34*, 1241–1253.

Mattioli, V., E. R. Westwater, D. Cimini, J. C. Liljegren, B. M. Lesht, S. I. Gutman, and F. J. Schmidlin (2007), Analysis of radiosonde and ground-based remotely sensed PWV data from the 2004 North Slope of Alaska Arctic winter radiometric experiment, *J. Atmos. Oceanic Tech.*, *24*, 415–430.

McMillin, L. M., M. Uddstrom, and A. Coletti (1992), A procedure for correcting radiosonde reports for radiation errors, *J. Atmos. Oceanic. Tech.*, *9*, 801–811.

McMillin, L. M., M. Gelman, A. Sanyal, and M. Sylva (1988), A method for the use of satellite retrievals as a transfer standard to determine systematic radiosonde errors, *Mon. Wea. Rev.*, *116*, 1091–1102.

Miloshevich, L. M., H. Vömel, D. N. Whiteman, B. M. Lesht, F. J. Schmidlin, and F. Russo (2006), Absolute accuracy of water vapor measurements from six operational radiosonde types launched during AWEX-G and implications for AIRS validation, *J. Geophys. Res.*, *111*, D09S10, doi:10.1029/2005JD006083.

Nash, J., R. Smout, T. Oakley, B. Pathack, and S. Kurnosenko (2006), WMO Intercomparison of Radiosonde Systems, Vacoas, Mauritius, 2–25 February 2005, WMO/TD-No. 1303,115 pp.

Nash, J., T. Oakley, H. Vömel, and W. Li (2011), WMO Intercomparison of High Quality Radiosonde Systems, Yangjiang, China, 12 July–3 August 2010. World Meteorological Organization, Instruments and Observing methods, report No. 107, 238 pp.

Randel, W. J., and F. Wu (2006), Biases in stratospheric and tropospheric temperature trends derived from historical radiosonde data, *J. Clim.*, *19*, 2094–2104.

Reale, A., B. Sun, F. Tilley, and M. Pettey (2012), NOAA Products Validation System (NPROVS), *J. Atmos. Oceanic. Tech.*, *29*, 629–645.

Seidel, D. J., B. Sun, M. Pettey, and A. Reale (2011), Global radiosonde balloon drift statistics, *J. Geophys. Res.*, *116*, D07102, doi:10.1029/2010JD014891.

Sun, B., A. Reale, D. J. Seidel, and D. C. Hunt (2010), Comparing radiosonde and COSMIC atmospheric profile data to quantify differences among radiosonde types and the effects of imperfect collocation on comparison statistics, *J. Geophys. Res.*, *115*, D23104, doi:10.1029/2010JD014457.

Sherwood, S. C., J. R. Lanzante, C. L. Meyer (2005), Radiosonde daytime biases and late-20th century warming, *Science*, 2 September 2005, *9*, 1556–1559.

Sherwood, S. C., C. L. Meyer, R. J. Allen, and H. A. Titchner (2008), Robust tropospheric warming revealed by iterative homogenized radiosonde data, *J. Clim.*, *21*, 5336–5352, doi:10.1175/2008JCL2320.1.

Sokolovskiy, S. (2003), Effect of superrefraction on inversions of radio occultation signals in the lower troposphere, *Radio Sci.*, *38*(3), 1058, doi:10.1029/2002RS002728.

Teweles, S., and F. G. Finger (1960), Reduction of diurnal variation in the reported temperatures and heights of stratospheric constant pressure surfaces, *J. Meteorol.*, *17*, 177–194.

Tarbell, T. C., and F. G. Tower (1980), Radiation corrections used in the AFGWC stratospheric analysis models, Rep. AFGWC/TN-80/004, 16 pp., U.S. Air Force, Air Weather Service (MAC), Air Force Global Weather Central, Offutt AFB.

Thorne, P. W., et al. (2011), A quantification of uncertainties in historical tropical tropospheric temperature trends from radiosondes, *J. Geophys. Res.*, *116*, D12116, doi:10.1029/2010JD015487.

Uddstrom, M. J. (1984), Solar radiation corrections for New Zealand and Australian radiosondes, *N. Z. Meteorol. Serv. Sci. Rep. 6*, 43 pp., New Zealand Meteorological Service, Wellington.